Grasp Analysis Using Deformable Fingers*

Matei Ciocarlie, Andrew Miller and Peter Allen
Department of Computer Science
Columbia University
New York, NY 10027 USA
{*cmatei, amiller, allen*}*@cs.columbia.edu*

***Abstract*— The human hand is unrivaled in its ability to grasp and manipulate objects, but we still do not understand all of its complexities. One benefit it has over traditional robot hands is the fact that our fingers conform to a grasped object's shape, giving rise to larger contact areas and the ability to apply larger frictional forces. In this paper, we demonstrate how we have extended our simulation and analysis system with finite element modeling to allow us to evaluate these complex contact types. We also propose a new contact model that better accounts for the deformations and show how grasp quality is affected. This work is part of a larger project to understand the benefits the human hand has in grasping.**

***Index Terms*— Grasp Analysis, Deformations, FEM**

I. Introduction

Evolution has provided humans with incredibly sophisticated means of manipulation. As an end-effector, the human hand is unrivaled. There is an inherent mismatch between the mechanical design and capabilities of robotic hands versus human hands, as robotics-based models use idealized simple joints, torque motors and finger-pad elements. As part of a larger project to understand the effect these differences have on a hand's ability to grasp, this paper focuses on modeling the deformations undertaken by fingers as they grasp rigid objects. This deformation is a key factor in the human hand's ability to create stable, encompassing grasps with subsets of fingers. Typical robot hands use stiff fingers that do not deform, and this often leads to difficulty in grasping.

Grasp analysis methods use a variety of contact models to describe the possible forces and torques that can be transmitted from one body to the other through the interface. When two rigid bodies contact at a point, there is always some amount of friction that can be supported within the tangent plane of the contact. If one of the bodies is deformable, then the contact will no longer occur at just a point but will be over some area that increases as the normal force increases. Then it is possible for the contact to support frictional moments about the contact normal as well, and the magnitude of these moments is constrained by the magnitude of the tangential friction and vice versa. In addition, contacts on soft fingertips are able to resist some disturbance moments within the contact tangent plane, which lead to further deformation of the fingertip and result in larger resistive moments.

* This work is supported by the National Science Foundation under Grant No. IIS-03-12693

To account for the complex nature of soft finger contacts, we have augmented the traditional model through Finite Element Analysis. After reviewing some of the previous work related to frictional contact models and deformable fingers, we will discuss the existing contact models and propose an improved model that accounts for the ability of a deformed finger to apply normal forces over an area larger than a point. In section IV, we show how the Finite Element Method can be used to analyze the characteristics of a soft contact, such as contact area shape and size, as well as frictional forces and moments. We also show how these characterstics affect the overall grasp quality. Section V describes how this work fits into our larger project of identifying and modeling the properties of a human hand that make it such an effective grasper. Finally, we present our conclusions and plans for future research.

These modeling and simulation efforts extend our previous research in grasp simulation using the *GraspIt!*[1] simulator, which can accommodate a wide variety of hand and robot designs [1], [2]. It includes a rapid collision detection and contact determination system that allows a user to interactively manipulate the joints of the hand and create new grasps of a target object. Each grasp is evaluated with numeric quality measures, and visualization methods allow the user to see the weak point of the grasp and create arbitrary 3D projections of the 6D grasp wrench space. The dynamics engine within *GraspIt!* computes the motions of a group of connected robot elements, such as an arm and a hand, under the influence of controlled motor forces, joint constraint forces, contact forces and external forces. This allows the dynamic simulation of an entire grasping task, as well as the ability to test custom robot control algorithms.

II. Related Work

Theoretical and experimental results have been presented in the analysis of soft finger contact models. Goyal et al. [3] present the concept of limit surface, characterizing the relationship between relative motion and frictional forces and moments for planar contacts. Howe and Cutkosky [4] discuss the shape of the limit surface for different contact pressure

[1]The source code for *GraspIt!* is available for download from http://www.cs.columbia.edu/~amiller/graspit.

distributions and develop practical methods for constructing the limit surface using experimental results. Xydas et al. proposed the power-law model for the contact between a soft fingertip and a rigid object [5], and used non-linear Finite Element simulations as well as experimental data to derive the parameters of the model for specific materials and fingertip shapes [6].

The effect that soft fingertips have on grasping and manipulation ability is discussed in [7], while specific fingertip materials and their impact on rolling manipulation tasks are discussed in [8]. Designing controllers for robotic fingers with soft tips has also been a highly active area of research. Reznik et al. [9] proposed a mass-spring model for deformable fingertips and design a controller able to interact with the model in real time. The problem of controlling a robotic finger when the dynamic properties of the soft fingertip are unknown is discussed in [10], using sensory feedback to design a controller that can learn the characteristics of the fingertip and apply the desired level of force on the grasped object. This method was also extended and applied for two-fingered grasps and manipulation tasks [11], while the control of rolling manipulation using deformable fingertips is discussed in [12].

The interaction between rigid and deformable objects has also been studied in order to recover contact forces for haptic feedback. Picinbono et al. [13] used the Finite Element Method to simulate human organs undergoing laparoscopic surgery. Duriez et al. [14] proposed a different Finite Element approach to obtain haptic feedback from manipulating a virtual deformable object.

Human finger deformation and its grasping ability have also been studied. Barbagli et al. proposed a soft finger proxy model of human fingers based on experimental data for use in haptic simulations [15]. This allows them to impart moments on an object grasped between two fingers without computing actual finger deformations which would degrade real-time performance. A Finite Element model of a human finger was used by biomedical engineering researchers [16] to investigate the behavior of mechanoreceptors that govern sense of touch under line loads while a viscoelastic model was used to predict fingertip pulp displacement during fast tapping [17].

III. Contact Models

Understanding the nature of contact is paramount to the analysis of grasping. When two objects touch, it is possible for each of them to transmit forces and velocities through the regions of contact. We will briefly discuss some possible contact models, using the following notations: a contact coordinate frame is defined with the origin in the pressure-weighted center of the contact region and with the z axis parallel with the contact normal direction $\hat{n}$. Total normal force applied at a contact is f_n. Contact frictional force is applied in a direction that is perpendicular to the contact normal and is given by f_t, while f_x and f_y represent its components along the x and y axes. Frictional moment is applied around the normal direction and is given by τ_z.

A. Point Contact with Friction

For point contacts, a commonly used model is point contact with friction or PCWF. The limit on the size of the tangential frictional forces that can arise at the contact is determined using Coulomb's model, and the contact can not resist any moment applied around its normal direction:

$$f_x^2 + f_y^2 \leq \mu^2 f_n^2 \quad (1)$$

$$\tau_z = 0 \quad (2)$$

From this equation, it is apparent that the forces that may be applied at the contact lie within a cone aligned with the contact normal, commonly known as a *friction cone*.

B. Soft Finger Contact

The situation becomes more complex once contacts can no longer be assumed to have zero area. When a deformable finger comes into contact with either a rigid body or another deformable body, the initial area may be only a point, but in a short time the contact begins to conform to the local shape of the contacted object. Friction arising at the contact can also resist moments about the contact normal, thus requiring a different contact model.

The Soft Finger Contact model, or SFC, uses the concept of a limit surface which we briefly describe below and further details can be found in [3], [4]. For a planar contact surface, assume instantaneous motion described as a pure rotation around a center of rotation, or COR, lying in the contact plane (COR is at infinity in the case of pure translation). Once the direction of relative motion at the contact is decided, the total frictional force and moment that are applied at the contact can be determined. The surface obtained by plotting the frictional force against the frictional moment computed for various positions of the COR is called the limit surface. It completely describes the space of forces and moments that contact friction can resist: if the point obtained by plotting a given force against a given moment lies inside the limit surface then slip will not occur. Steady sliding will occur if the point is on the limit surface, and sliding will accelerate if the point lies on its outside.

Expressions for frictional force and moment depend on the pressure distribution inside the contact, and analytical solutions exist only for a few special cases, such as Hertzian or uniform pressure. However, it was shown [4] that for most pressure distributions the limit surface can be approximated by an ellipsoid. This shows that the magnitudes of the maximum frictional tangential forces and axial moments are inter-related such that as the tangential force increases, the moment about the contact normal decreases. If no frictional

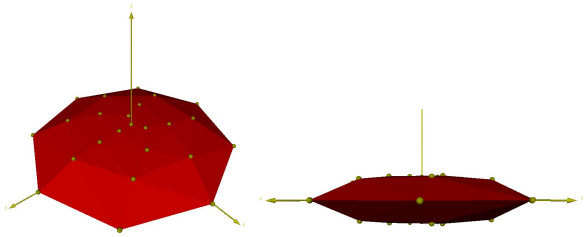

Fig. 1. These are two views of the friction ellipsoid with $e_z = 0.2$, linearized by taking the convex hull of 40 points on its surface. The x and y axes show the magnitude of the respective components of tangential frictional force while the z axis shows the relative magnitude of the frictional moment.

moment is applied at the contact ($\tau_z = 0$) the total frictional force that can be applied in any direction in the tangent plane is equal to the total normal force multiplied by the coefficient of friction. The base of the ellipsoid is therefore always a circle with radius μf_n and the ellipsoid model is described by the relationship:

$$f_x^2 + f_y^2 + \frac{\tau_z^2}{e_z^2} \leq \mu^2 f_n^2 \tag{3}$$

where e_z^2 is the eccentricity parameter that relates the maximum value of τ_z to the friction coefficient μ and the normal force f_n: the maximum frictional moment $max(\tau_z) = e_z\,\mu\,f_n$ can be applied at the contact if tangential frictional forces are equal to 0 (see fig. 1). This parameter is set according to the characteristics of the contact area, such as shape, size and pressure distribution.

C. Soft Finger with Finite Contact Area

When using an accurate value of the eccentricity parameter e_z, the Soft Finger Model accurately describes the space of frictional forces and moments that a soft contact can apply. As the contact area shape and pressure distribution are not explicitly computed, the normal force applied at the contact is assumed to be concentrated in a single point, most likely the initial point of contact between the two surfaces. This means that the contact cannot resist moments that lie within the contact tangent plane. However, we feel that this is too conservative. These moments, as well as any other forces or moments resisted by the contact, will deform the finger and allow some motion, but the pressure distribution will change in response and ultimately limit that motion.

The method we propose for modeling soft finger contacts relies upon the Finite Element Method to compute the deformation of a soft fingertip in contact with a planar rigid surface. Given the value of the total normal force applied at the contact, we compute the contact forces applied at each vertex of the finite element mesh that prevent interpenetration, as well as the deformation of the soft fingerpad (the displacement of each vertex) as a result of contact. If relative motion at the contact is specified (by specifying the position of the COR) frictional forces that result during sliding will also be computed, as well as deformation due to these forces. Specific details regarding the derivation and implementation of the finite element simulation method can be found in Appendix I.

Using the contact area information resulting from the finite element simulation, we augment the space of forces and moments that the contact can apply with the range of moments obtained by considering the contribution of the total normal force applied at any of the vertices comprised in the contact area. This range is added to the space of frictional forces and moments created using a Soft Finger Contact model positioned at the center of pressure. We now have a complete model of the contact that can be used for grasp analysis, as discussed in the next section.

IV. Grasp Analysis

A. Grasp Quality Metrics

Our aim is to examine the ability of a grasp to maintain relative object position in the face of disturbances. We refer to the complete range of wrenches that a grasp can apply as the grasp wrench space. We will briefly describe the method used for the construction of the grasp wrench space, and for further details we refer the reader to [18]. In order to obtain coherent results that can be used to compare grasps applying a wide range of normal forces, the value of the total normal force applied at each contact is scaled to 1. The process then assumes that the space of frictional forces at each contact can be represented with a finite set of friction wrenches. For each of these, an object wrench is computed based on the contact location relative to a common reference point within the body. The total grasp wrench space is computed by finding the Minkowski sum of the sets of object wrenches $(\boldsymbol{w}_{i,1}, \ldots, \boldsymbol{w}_{i,m})$ associated with each of the n contacts, and then taking the convex hull of the resulting set:

$$GWS_{L_\infty} = ConvexHull(\bigoplus_{i=1}^{n}\{\boldsymbol{w}_{i,1}, \ldots, \boldsymbol{w}_{i,m}\}). \tag{4}$$

The Minkowski sum operation allows us to consider the independent contributions of contacts on different fingers, but it quickly becomes intractable for large numbers of contacts. One approximation is to simply use the union of the contact wrenches instead, or if we are interested in a particular portion of the wrench space, we can first build a coarse model of the space using fewer contact wrenches, and then incrementally refine it, as in [19].

We will use the total volume of the resulting wrench space as a quality metric that allows different grasps to be compared. Another possible metric is the smallest distance between the origin and the boundary of the wrench space, which determines the magnitude of the worst-case wrench that the grasp can resist. Both of these metrics, inferred using

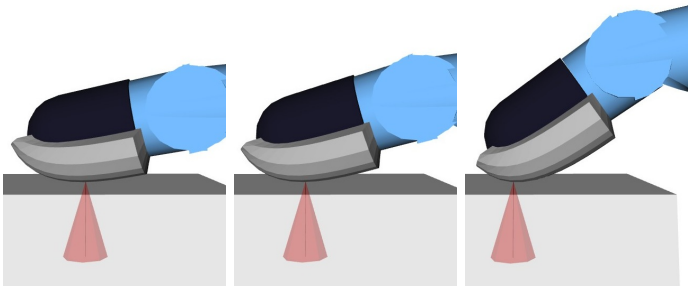

Fig. 2. Three possible contacts between a soft fingerpad and a rigid planar surface. Left: low local curvature ("flat" contact); Middle: medium local curvature; Right: high local curvature ("round" contact)

the total grasp wrench space, rely on a correct model for the space of forces that each participating contact can apply.

B. Frictional Forces and Moments

We use the ellipsoidal approximation for the limit surface described in section III-B to create the space of frictional forces and moments that can be applied at each contact. The eccentricity parameter e_z that defines the ellipsoid can be obtained experimentally [4], but the resulting value is only accurate for the particular combination of normal force and finger structure used in the experiment. For example, it has been shown [15] that if the contact area varies with the applied normal force, the relationship between $max(\tau_z)$ and f_n is non-linear, which implies that the value of e_z changes with variations in the normal force.

Using the FEM-based simulation we can compute the total frictional force and moment applied at the contact for any relative motion between the bodies in contact. Any such force-moment combination describes a point on the limit surface, therefore the entire limit surface can be plotted by sampling these values for different positions of the COR. Of particular interest is the maximum frictional torque $max(\tau_z)$ that can applied at the contact for a given normal force f_n. This value is equal to the frictional torque applied with the COR positioned at the pressure-weighted center of the contact area, and the eccentricity parameter can be recovered as $e_z = \frac{max(\tau_z)}{f_n}$.

To illustrate this method we have modeled the contact between a robotic finger with a soft fingerpad and a rigid planar surface. We chose three contact locations on the fingerpad, each with a different local curvature (figure 2), leading to different pressure distributions inside the contact area. At each of these contact points we used the finite element method to compute maximum frictional torque for a range of applied normal forces. The results are shown in figure 3: the finite element simulation captures the non-linearities between $max(\tau_z)$ and f_n for small normal forces, and displays an almost linear relationship in the upper range of normal forces. This is explained by the fact that as normal

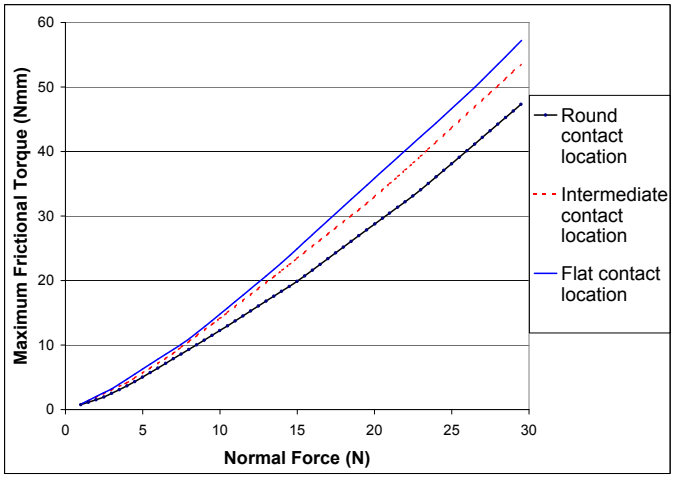

Fig. 3. Maximum frictional torque vs. total normal force for three contact locations: "flat", "intermediate" and "round", in the order of increasing local curvature of the fingerpad

forces increase, the contact area eventually reaches a plateau where even large forces do not affect the surface of contact.

Figure 3 also shows that the linear region of each of the three plots displays a different inclination. This is an expected result, as the shape and size of the stabilized contact area will vary depending on the location of the contact on the fingertip, with larger contact areas created on flat regions and smaller areas on regions with high curvature. In consequence, a contact established in the flat region of the finger is able to apply a higher torque than a contact in a region with higher curvature applying equal normal force.

We conclude that the finite element simulation can be used to predict the value of the parameter e_z for different contact locations and normal forces, allowing the construction of the friction ellipsoid corresponding to each contact.

C. Moments Corresponding to Normal Forces

We complete the model of the contact wrench space by adding object wrenches corresponding to unit forces applied along the contact normal at each of the vertices of the contact surface. Computation can be simplified by observing that it suffices to consider the wrenches introduced by placing the normal force at the vertices that form the boundary of the surface (i.e. any wrench resulting from a force applied at a position inside this area will be comprised in the convex hull of the boundary wrenches). Total contact wrench space is then constructed by applying the convex hull operation on the complete set of contact wrenches, including the contributions of frictional and normal forces.

The total grasp wrench space is constructed as discussed in section IV, by taking the convex hull of the Minkowski sum of all contact wrench spaces. We can now compute the quality metric of a grasp, as discussed in the following section.

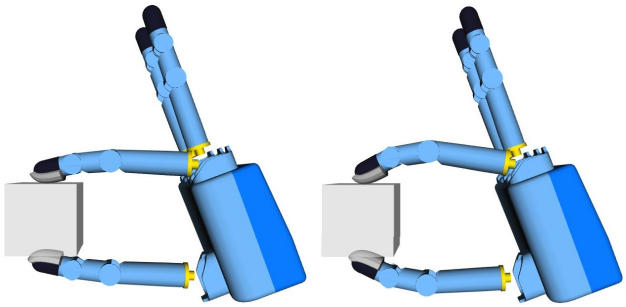

Fig. 4. The DLR hand grasping a cube with two fingers, using different locations of the fingerpad. Left: flat contact region; Right: round contact region

TABLE I

GRASP QUALITIES AT DIFFERENT POSITIONS ON THE FINGERPAD

Fingerpad curvature at contact locations	Grasp quality
low	0.893
intermediate	0.828
high	0.778

D. Results

We have used this method to compute the quality metric of three grasps, with the DLR hand using two fingers with soft fingerpads to grasp a cube. These fingerpads have an elasticity modulus of 0.8 MPa, corresponding to soft rubber. All three grasps applied the same total normal force at each contact. However, the location of the contact on the fingerpads was different between each grasp, with both fingers creating either "flat", "round" or "intermediate" contacts. A comparative view of two of these grasps is shown in figure 4, and the quality metric for each grasp is presented in table I. As expected, the best grasp is the one that uses the flat regions of the fingertip, with quality decreasing for the grasps that use fingerpad regions with higher local curvature.

We also analyzed the relationship between grasp quality and normal force applied at the contacts. Figure 5 shows the quality of the grasp for a range of normal contact forces, using flat fingerpad contact locations. As mentioned before, contact normal forces are scaled to 1 for the grasp quality computation. When this method is applied to rigid fingers, the resulting quality value is therefore independent of the applied normal forces. However, for soft fingers, when an increase in normal force causes an increase in contact area size, grasp quality is also affected. This is explained by the increase of the eccentricity parameter e_z of the friction ellipsoid, which, as discussed in section III-B, shows the ratio of contact frictional moment to normal force. Once the contact area stabilizes, the eccentricity parameter also approaches a constant value, therefore grasp quality does not grow significantly even with further increases of contact normal forces. In figure 6 we show the deformation of the

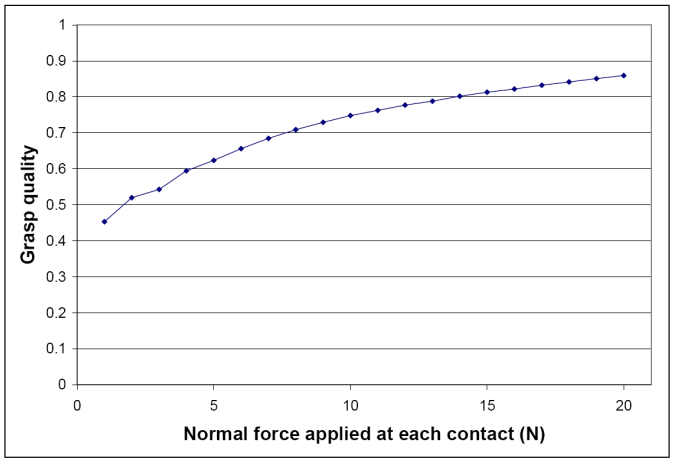

Fig. 5. Grasp quality vs. normal force applied at each contact

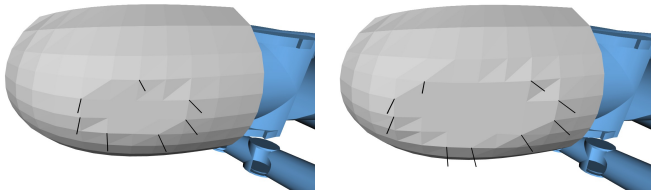

Fig. 6. The contact area grows quickly after the initial contact is made. Here we show a view of the contact areas for a 5N normal force (left) and a 25N normal force (right) from within a transparent cube. The vertices of the convex boundary of the contact area are marked with thin cylinders.

index finger that was computed for normal forces of 5N and 25N.

The results of this grasp analysis method are qualitatively correct, however quantitative validation can only be performed by comparing simulation results with experimental data. Various aspects of the simulation can be tested experimentally, such as the value of the eccentricity parameter e_z for varying finger structures and materials, or the magnitude of the worst-case disturbance that can be resisted by a contact. We intend to perform such analysis as part of future development.

V. HUMAN HAND

Our current efforts are focused on constructing a biomechanically realistic human hand model. Such a model would serve to aid clinicians planning reconstructive surgeries of a hand, since many of the mechanical aspects of this complex organ are still not fully understood. However, this sort of model would also allow us to determine which features of the human hand are the most important to be mimicked when designing a robotic hand. These beneficial features will be identified by creating several versions of the human hand model, each with different sets of features, and analyzing the ability of each hand to perform a set of grasping and manipulation tasks. The iterative refinements include skin

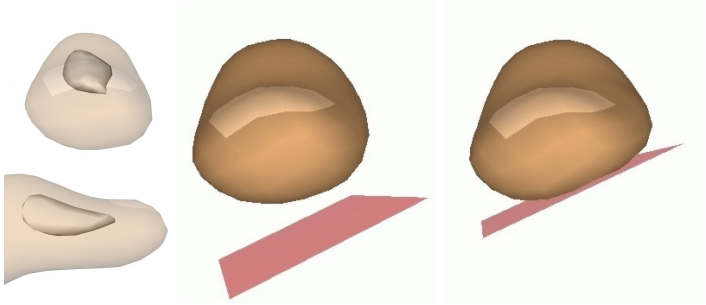

Fig. 7. Left: Front and Side views of a human thumb model constructed using CT data. Middle and Right: A planar surface is pushed up into the thumb pad which deforms in response. Notice the bulges on the sides of the thumb due to the nearly incompressible nature of human tissue.

deformations, realistic human joints to determine the benefits of a compliant kinematic structure, and the network of tendons to determine what are the advantages, if any, of indirect actuation of the joints [20].

In order to study the behavior of the human fingertip during grasping we are using the FEM to simulate loads applied to a human thumb. To generate a highly realistic model we are using a set of Computed Tomography (CT) scans of a real thumb. The data comes in the form of cross-sectional slices showing the contours of both soft tissue and bone. Specialized software is used to process these slices and obtain 3D surface information on the outer shape of the finger and the bone inside, and surface information is further processed in order to generate a finite element mesh. The final model consists of 332 nodes and 1007 finite elements (tetrahedra) and the value of the elastic modulus of human tissue is set using the results of [16]. Simulation results are shown in figure 7. We are currently investigating methods to validate these results by studying the ratio of load to contact surface and comparing it to real-life data. Future work will also assess how the simulation of multiple tissue layers affects these results.

VI. Conclusion and Future Work

We consider that the analysis method presented in this paper can capture the effect that compliant contact surfaces have on soft-fingered grasps. With an increased contact region, fingers are able to apply forces over a larger area and thus are able to apply a greater variety of moments to the grasped object. This is taken into account by the grasp analysis, which uses a Soft Finger Contact model to describe the space of contact frictional forces and moments, and a finite element based simulation to recover contact specific parameters and pressure distributions. We believe that the use of the FEM provides us with a framework for building highly realistic models for a wide range of complex-structured fingers.

In its current version, this method is limited to grasp analysis for situations in which all the contacts involved are planar. This is due in equal measure to the Soft Finger friction model and the finite element simulator, both of them restricted to planar contacts. We plan to build on the work presented in this paper with the goal of delivering a grasp analysis method for deformable fingers that can be applied to grasps involving non-planar contacts and a wide variety of finger structures and grasped objects.

Acknowledgments

We would like to thank Professor Gerd Hirzinger and Dr. Max Fischer from the German Aerospace Center (DLR) for providing us with models of their robotic hand. We thank the members of the Cornell Neuromuscular Biomechanics Lab (Professor Francisco Valero-Cuevas, Veronica Santos, and Alex Deyle) and Dr. Douglas Mintz from the Hospital for Special Surgery in NY for their help in obtaining the CT scanned finger data. Finally, we would also like to thank Professor Eitan Grinspun for his help with the FEM formulation.

Appendix I
Modeling deformable fingertips using the Finite Element Method

Our method for simulating frictional contact between a soft fingertip and a planar rigid surface is based primarily on [21] and a brief description is given below. We assume familiarity with the basic concepts of the stress-strain approach to FEM, as described in textbooks such as [22].

Given the total normal force applied at the contact as well as relative motion of the two bodies, we would like to compute the deformation of the fingertip as well as the contact forces applied at each vertex that cause this deformation. Consider a vertex of the deformable mesh that makes contact with the planar surface. We will decompose the contact force applied at this vertex into a component normal to the rigid plane and a tangential component. The value of the normal component will be given by $\boldsymbol{f}_i^n = \lambda_i \hat{\boldsymbol{n}}_i$ where the scalar λ_i represents the unknown magnitude of the normal force applied at vertex i and $\hat{\boldsymbol{n}}_i$ is the surface normal. We will refer to this normal component as contact traction. The tangential component of the contact force appears as a result of contact friction. Using a Coulomb friction model, the magnitude and direction of this component are given by $\boldsymbol{f}_i^t = \mu\lambda_i\hat{\boldsymbol{v}}_i$ where the normalized vector $\hat{\boldsymbol{v}}_i$ represents the direction of relative velocity at the vertex i.

The complete vector of nodal contact forces $\boldsymbol{r}_c$ can be assembled using the above expressions, with one entry for each contact node:

$$\boldsymbol{r}_c = \left[\ldots, \lambda_i \left(\hat{\boldsymbol{n}}_i + \mu\hat{\boldsymbol{v}}_i\right)^T, \ldots\right]^T \tag{5}$$

where $\lambda_i \left(\hat{\boldsymbol{n}}_i + \mu\hat{\boldsymbol{v}}_i\right)$ is the total contact force manifested at vertex number i.

For each contact vertex we therefore introduce a new unknown, the magnitude of contact traction λ_i. Further constraints need to be imposed on this set of unknowns: contact traction must prevent interpenetration without adding energy to the system. For any vertex i of the deformable mesh we define the gap function g_i as the signed distance between the position of the vertex and the contact plane. The above constraint can be expressed as:

$$g_i \geq 0, \lambda_i \geq 0, g_i \lambda_i = 0 \tag{6}$$

This formulation ensures that no interpenetration is occurring ($g_i \geq 0$), contact forces can only push (not pull) deformable vertices ($\lambda_i \geq 0$) and contact tractions can only be applied at contact vertices for which the gap is equal to zero ($g_i \lambda_i = 0$). In practice, we enforce these constraints using a function that closely approximates equations (6) but is differentiable as required by the Newton iteration method. One example is

$$w(g, \lambda) = \frac{g + \lambda}{2} - \sqrt{\left(\frac{g - \lambda}{2}\right)^2 + \epsilon} \tag{7}$$

which has the property that for very small but nonzero ϵ the solutions of $w(g, \lambda) = 0$ have the required characteristics. Again we assemble these constraints into a global constraint vector $\boldsymbol{f}_c$ with one entry for each deformable vertex:

$$\boldsymbol{f}_c = [\ldots, w(g_i, \lambda_i), \ldots] \tag{8}$$

The complete equilibrium conditions with contact constraints are:

$$\boldsymbol{K}\boldsymbol{u} = \boldsymbol{f} + \boldsymbol{r}_c \tag{9}$$

$$\boldsymbol{f}_c = 0 \tag{10}$$

where $\boldsymbol{K}$ is the body stiffness matrix, $\boldsymbol{f}$ contains any additional forces (such as gravity) that may act on the vertices and $\boldsymbol{u}$ is the vector of nodal displacements. We can now solve for nodal displacements and contact nodes traction using the Newton iteration method to account for non-linear dependencies of the stiffness matrix $\boldsymbol{K}$ on $\boldsymbol{u}$.

REFERENCES

[1] A. Miller and H. Christensen, "Implementation of multi-rigid-body dynamics within a robotic grasping simulator," in *Proc. of the 2003 IEEE Intl. Conf. on Robotics and Automation*, 2003, pp. 2262–2268.

[2] A. Miller and P. K. Allen, "Graspit!: A versatile simulator for robotic grasping," *IEEE Robotics and Automation Magazine*, vol. 11, no. 4, pp. 110–122, December 2004.

[3] S. Goyal, A. Ruina, and J. Papadopoulos, "Planar sliding with dry friction, part 1," *Wear*, vol. 143, pp. 307–330, 1991.

[4] R. Howe and M. Cutkosky, "Practical force-motion models for sliding manipulation," *Intl. J. of Robotics Research*, vol. 15, no. 6, pp. 557–572, December 1996.

[5] N. Xydas and I. Kao, "Modeling of contact mechanics with experimental results for soft fingers," in *IEEE Intl. Conf. on Intelligent Robots and Systems*, 1998, pp. 488–493.

[6] N. Xydas, M. Bhagavat, and I. Kao, "Study of soft-finger contact mechanics using finite elements analysis and experiments," in *IEEE Intl. Conf. on Robotics and Automation*, 2000, pp. 2179–2184.

[7] K. B. Shimoga and A. A. Goldenberg, "Soft materials for robotic fingers," in *IEEE Intl. Conf. on Robotics and Automation*, 1992, pp. 1300–1305.

[8] D. C. Chang and M. R. Cutkosky, "Rolling with deformable fingertips," in *IEEE Intl. Conf. on Intelligent Robots and Systems*, 1995, pp. 2194–2199.

[9] D. Reznik and C. Laugier, "Dynamic simulation and virtual control of a deformable fingertip," in *IEEE Intl. Conf. on Robotics and Automation*, April 1996, pp. 1669–1674.

[10] Z. Doulgeri, A. Simeonidis, and S. Arimoto, "A position/force control for a soft tip robotic finger under kinematic uncertaintes," in *IEEE Intl. Conf. on Robotics and Automation*, 2000, pp. 3867–3872.

[11] H. Y. Han, S. Arimoto, K. Tahara, M. Yamaguchi, and P. Nguyen, "Robotic pinching by means of a pair of soft fingers with sensory feedback," in *IEEE Intl. Conf. on Robotics and Automation*, 2001, pp. 97–102.

[12] Z. Doulgeri and J. Fasoulas, "Grasping control of rolling manipulations with deformable fingertips," *IEEE/ASME Transactions on Mechatronics*, vol. 8, no. 2, pp. 283–286, 2003.

[13] G. Picinbono, J. Lombardo, H. Delingette, and N. Ayache, "Improving realism of a surgery simulator: Linear anisotropic elasticity, complex interactions and force extrapolation," *J. Visualization and Computer Animation*, 2002.

[14] C. Duriez and C. Andriot, "A multi-threaded approach for deformable/rigid contacts with haptic feedback," in *12th Intl. Symposium on Haptic Interfaces for Virtual Environments and Teleoperator Systems*, 2004, pp. 272–279.

[15] F. Barbagli, A. Frisoli, K. Salisbury, and M. Bergamasco, "Simulating human fingers: a soft finger proxy model and algorithm," in *12th Intl. Symposium on Haptic Interfaces for Virtual Environments and Teleoperator Systems*, 2004, pp. 9–17.

[16] K. Dandekar, B. Raju, and M. Srinivasan, "3-D finite-element models of human and monkey fingertips to investigate the mechanics of tactile sense," *J. Biomechanical Engineering*, 2003.

[17] D. Jindrich, Y. Zhou, T. Becker, and J. Dennerlein, "Non-linear viscoelastic models predict fingertip pulp force-displacement characteristics during voluntary tapping," *Journal of Biomechanics*, vol. 36, pp. 497–503, 2003.

[18] C. Ferrari and J. Canny, "Planning optimal grasps," in *Proc. of the 1992 IEEE Intl. Conf. on Robotics and Automation*, 1992, pp. 2290–2295.

[19] C. Borst, M. Fischer, and G. Hirzinger, "A fast and robust grasp planner for arbitrary 3D objects," in *Proc. of the 1999 IEEE International Conference on Robotics and Automation*, Detroit, MI, May 1999, pp. 1890–1896.

[20] F. Valero-Cuevas, "Applying principles of robotics to understand the biomechanics, neuromuscular control and clinical rehabilitation of human digits," in *Proc. of the 2000 IEEE Intl. Conf. on Robotics and Automation (2000)*, 2000, pp. 255–262.

[21] A. Eterovic and K. Bathe, "On the treatment of inequality constraints arising from contact conditions in finite element analysis," *Computers and Structures*, vol. 40, no. 2, pp. 203–209, 1991.

[22] O. Zienkiewicz and R. Taylor, *The Finite Element Method*, 4th ed. McGraw-Hill, 1989.